

Motivation

Problem
statement

Methods

Bayesian
inference

Structural
analysis

Reduced basis
approximation

Results

RB results

Damage
scenarios

Computational
times

Summary
and
conclusions

Future work

Digital twin-driven statistical fatigue life prediction of a damaged structure

Dayoung Kang

Department of Aerospace Engineering

Oct 20, 2023

Digital twin

- Virtual replica of a physical system
- Three main components: Physical entity, digital entity, and data stream

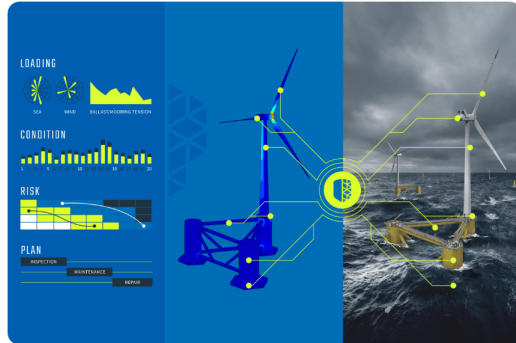


Figure 1: Digital twin example: wind turbine

- Diagnose the status of a defect by updating a virtual model based on sensor data of a physical asset
- Realize condition-based monitoring (CBM) that improve safety and reduce operating costs at the same time

Motivation

Problem statement

Methods

Bayesian inference
Structural analysis
Reduced basis approximation

Results

RB results
Damage scenarios
Computational times

Summary and conclusions

Future work

Target application: High-pressure hydrogen storage vessel for hydrogen refueling station

- Exposed to various damage sources that can cause physical defects during the transportation and loading/unloading
- Relieve safety concerns by monitoring damaged pressure vessel
- From periodic maintenance (expensive) to only when needed

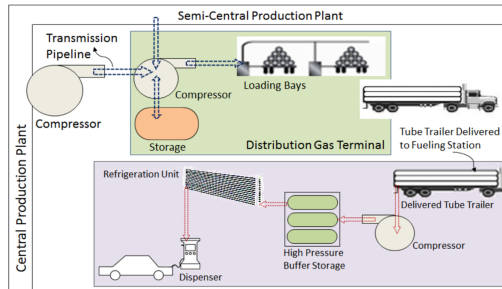


Figure 2: Storage, transportation, and charging process of a vessel[†]

[†] Reddi, K., Mintz, M., Elgowainy, A., & Sutherland, E. (2016). Challenges and opportunities of hydrogen delivery via pipeline, tube-trailer, LIQUID tanker and methanation-natural gas grid. Hydrogen science and engineering: materials, processes, systems and technology, 849-874.

Motivation

Problem statement

Methods

Bayesian inference
Structural analysis
Reduced basis approximation

Results

RB results
Damage scenarios
Computational times

Summary and conclusions

Future work

Previous research

- ① Digital twin based on a finite element (FE) model
 - Accurate but computationally expensive
 - Not ideal for digital twin application
- ② Reduced basis (RB) method[†]
 - Physics-driven reduced-order modeling
 - Achieve a significant reduction in computational time

Goal

Digital twin-driven fatigue life prediction of a defected vessel using RB method

[†]Hesthaven, J. S., Rozza, G., & Stamm, B. (2016). Certified reduced basis methods for parametrized partial differential equations (Vol. 590). Berlin: Springer.

Goal: predict number of cycles to failure N_f for condition-based maintenance

- Estimate N_f as the dent size grows
- Consider uncertainties in system parameters $\mu = (E, \nu, p, d)$
 E : Young's modulus, ν : Poisson's ratio, p : internal pressure, d : dent size
- $N_f = f(\underbrace{E, \nu, p, d}_{\text{unknowns}})$, unknowns must be estimated from strain data y_o

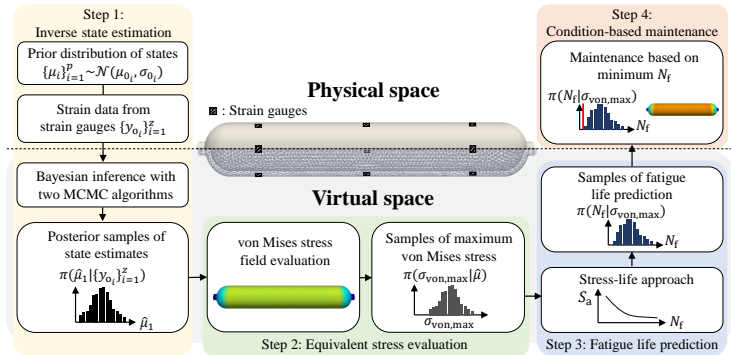


Figure 3: Overview of a fatigue life prediction using digital twin

Motivation

Problem
statement

Methods

Bayesian
inferenceStructural
analysisReduced basis
approximation

Results

RB results

Damage
scenariosComputational
timesSummary
and
conclusions

Future work

- Bayesian inference
 - Infer unknown system states (parameters) in the form of posterior distribution based on strain measurement

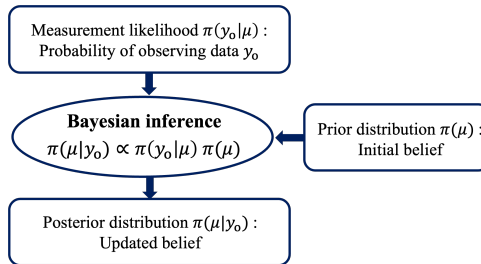


Figure 4: Concept of a Bayesian inference

- Markov-Chain Monte Carlo (MCMC) simulation[†]
 - Samples parameters from the posterior distribution
 - Computationally expensive due to large number of evaluations

[†] Stark, P. B., & Tenorio, L. (2010). A primer of frequentist and Bayesian inference in inverse problems. Large-scale inverse problems and quantification of uncertainty, 9-32.

Methods

Structural analysis model

- Model configuration



Figure 5: Damaged pressure vessel model

- Boundary conditions

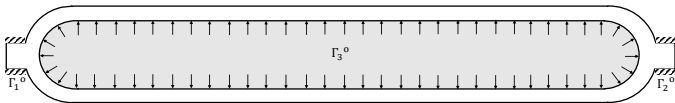


Figure 6: Boundary conditions of a damaged vessel model

- High-fidelity FE system

$$A_{\mathcal{N}}(\mu)u_{\mathcal{N}}(\mu) = f_{\mathcal{N}}(\mu)$$

$A_{\mathcal{N}}(\mu) \in \mathbb{R}^{\mathcal{N} \times \mathcal{N}}$: Stiffness matrix

$u_{\mathcal{N}}(\mu) \in \mathbb{R}^{\mathcal{N}}$: FE solution (displacement) vector

$f_{\mathcal{N}}(\mu) \in \mathbb{R}^{\mathcal{N}}$: Load vector

Reduced basis approximation

FE system

$$A_{\mathcal{N}}(\mu)u_{\mathcal{N}}(\mu) = f_{\mathcal{N}}(\mu) \quad (1)$$

Idea: Approximate Equation (1) in $\text{span}(B)$

$B \in \mathbb{R}^{\mathcal{N} \times N}$: Reduced basis function matrix ($N \ll \mathcal{N}$)

Approximate solution

$$u_{\mathcal{N}}(\mu) \approx Bu_N(\mu) \quad (2)$$

$u_N(\mu) \in \mathbb{R}^N$: Reduced basis solution vector

Through Galerkin projection to Equation 1,

$$B^T A_{\mathcal{N}}(\mu) B u_N(\mu) = B^T f_{\mathcal{N}}(\mu) \quad (3)$$

Here, for computational efficiency, RB does affine decomposition,

$$\underbrace{\sum_{q=1}^{Q_a} \theta_a^q(\mu) \underbrace{B^T A_{\mathcal{N}}^q B}_{\text{offline}} u_N(\mu)}_{\text{online}} = \sum_{q=1}^{Q_f} \theta_f^q(\mu) \underbrace{B^T f_{\mathcal{N}}^q}_{\text{offline}}$$

$\theta_a^q(\mu), \theta_f^q(\mu)$: parameter μ -dependent functions

Results

RB results

From FE dimension $\mathcal{N} = 251,715$, reduced to $N = 48$.

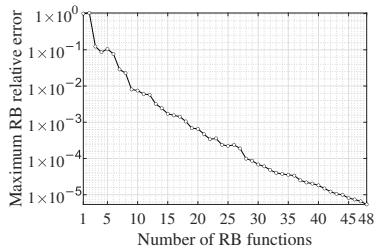


Figure 7: Error convergence for RB training

Using a total of 625 parameter samples,

Table 1: RB model verification compared to FE model

Output	Relative error (%)	
Displacement norm	Min.	1.59×10^{-6}
	Avg.	3.08×10^{-2}
	Max.	7.70×10^{-2}
von Mises stress	Min.	1.80×10^{-6}
	Avg.	4.98×10^{-2}
	Max.	1.25×10^{-1}

Motivation

Problem statement

Methods

Bayesian inference

Structural analysis

Reduced basis approximation

Results

RB results

Damage scenarios

Computational times

Summary and conclusions

Future work

Scenario 1: vessel with initially identified dent size $d=1$ cm

- Number of MCMC samples: 10^4
- Truth: $\mu_d = 1$ cm

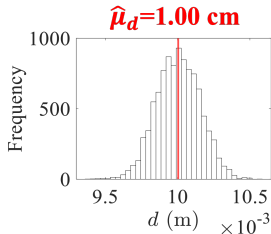


Figure 8: Posterior states estimates of a dent size for scenario 1

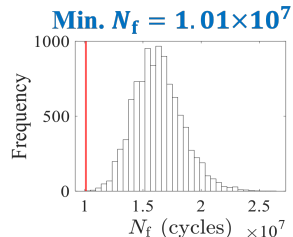


Figure 9: Number of cycles to failure for scenario 1

Motivation

Problem statement

Methods

Bayesian inference

Structural analysis

Reduced basis approximation

Results

RB results

Damage scenarios

Computational times

Summary and conclusions

Future work

Scenario 2: vessel with enlarged dent size $d=3$ cm

- Number of MCMC samples: 10^4
- Truth: $\mu_d = 3$ cm

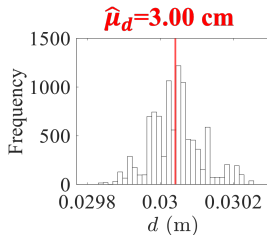


Figure 10: Posterior states estimates of a dent size for scenario 2

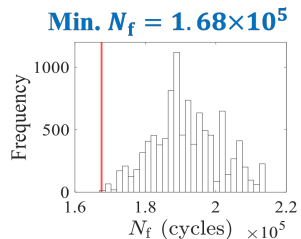


Figure 11: Number of cycles to failure for scenario 2

Achieved rapid simulations by significantly reducing the dimension

- From FE dimension $\mathcal{N} = 251,715$ to RB dimension $N = 48$ (Reduction rate: 5.24×10^3)

Offline/online computational time

- Single evaluation times

Table 2: Comparison of single evaluation times between FE and RB models

	FE model	RB model	Speed up
Offline time	-	2 hr 33 min	-
Averaged online time	1 min 44 s	1.59×10^{-4} s	6.52×10^5

- Total evaluation times for inverse state estimation

Table 3: Comparison of total evaluation times between FE and RB models

FE analysis time	RB analysis time	Speed up
41 days 12 hr 13 min	2 min 53 s	2.07×10^4

Motivation

Problem
statement

Methods

Bayesian
inferenceStructural
analysisReduced basis
approximation

Results

RB results

Damage
scenariosComputational
timesSummary
and
conclusions

Future work

Summary

- Proposed a statistical fatigue life monitoring scheme that relies on an RB digital twin
 - ① Inverse state estimation
 - ② Equivalent stress evaluation
 - ③ Fatigue life prediction
 - ④ Condition-based maintenance (CBM)
- The proposed strategy is demonstrated with a damaged pressure vessel.
- Thanks to the RB digital twin, entire process was accelerated compared to FE digital twin while retaining accuracy.

Conclusion

- Proposed fatigue life monitoring strategy assisted with an RB digital twin has shown to be effective for the CBM of a damaged structure.

Overcome challenges of model updating by using a component-based approach

- Effectively update a model by replacing a component with a defected component after identifying new damage locations

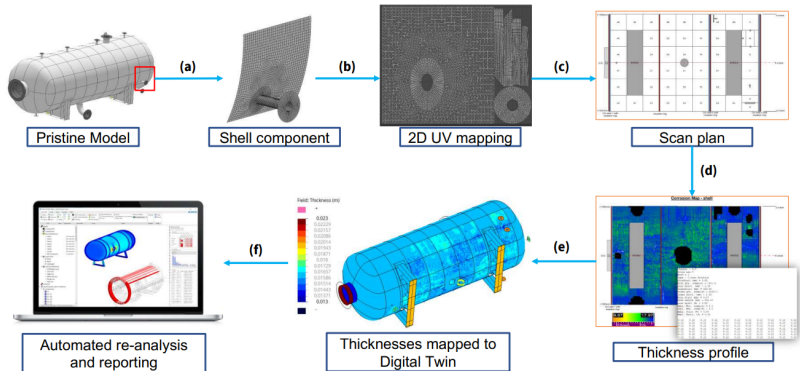


Figure 12: Digital twin of a pressure vessel using a component-based approach[†]

[†] Akseles, Case study: digital twin of pressure vessel, <https://www.akseles.com/resources-detail/digital-twins-of-pressure-vessels-unlocking-the-full-potential-of-ogtcs-robotic-inspection-joint-industry-project-with-the-oil-and-gas-technology-center>

Thank you

References

- [1] Reddi, K., Mintz, M., Elgowainy, A., & Sutherland, E. (2016). Challenges and opportunities of hydrogen delivery via pipeline, tube-trailer, LIQUID tanker and methanation-natural gas grid. *Hydrogen science and engineering: materials, processes, systems and technology*, 849-874.
- [2] Febrianto, E., Butler, L., Girolami, M., & Cirak, F. (2022). Digital twinning of self-sensing structures using the statistical finite element method. *Data-Centric Engineering*, 3, e31.
- [3] Ramancha, M. K., Astroza, R., Conte, J. P., Restrepo, J. I., & Todd, M. D. (2020). Bayesian nonlinear finite element model updating of a full-scale bridge-column using sequential monte carlo. In *Model Validation and Uncertainty Quantification, Volume 3* (pp. 389-397). Springer, Cham.
- [4] Wang, T., Liu, Z., Liao, M., & Mrad, N. (2020, November). Life prediction for aircraft structure based on Bayesian inference: towards a digital twin ecosystem. In *Annual Conference of the PHM Society* (Vol. 12, No. 1, pp. 8-8).
- [5] Fang, X., Wang, H., Li, W., Liu, G., & Cai, B. (2022). Fatigue crack growth prediction method for offshore platform based on digital twin. *Ocean Engineering*, 244, 110320.
- [6] Karve, P., Guo, Y., Kapusuzoglu, B., Mahadevan, S., & Haile, M. (2020, November). Digital twin approach for intelligent operation planning and health management of mechanical systems. In *Annual Conference of the PHM Society* (Vol. 12, No. 1, pp. 1-9).
- [7] Hesthaven, J. S., Rozza, G., & Stamm, B. (2016). Certified reduced basis methods for parametrized partial differential equations (Vol. 590). Berlin: Springer.

References

Motivation

Problem
statement

Methods

Bayesian
inference

Structural
analysis

Reduced basis
approximation

Results

RB results

Damage
scenarios

Computational
times

Summary
and
conclusions

Future work

- [8] Stark, P. B., & Tenorio, L. (2010). A primer of frequentist and Bayesian inference in inverse problems. Large-scale inverse problems and quantification of uncertainty, 9-32.
- [9] Kang, S., & Lee, K. (2021). Real-time, high-fidelity linear elastostatic beam models for engineering education. Journal of Mechanical Science and Technology, 35(8), 3483-3495.
- [10] The American Society of Mechanical Engineers, ASME Boiler & Pressure Vessel Code, Section VIII Division 2, 2019 Edition
- [11] Akselos, Case study: digital twin of pressure vessel, <https://www.akselos.com/resources-detail/digital-twins-of-pressure-vessels-unlocking-the-full-potential-of-ogtcs-robotic-inspection-joint-industry-project-with-the-oil-and-gas-technology-center>

Fatigue
analysis

Linear
elasticity
problem

Geometric pa-
rameterization

Empirical
interpolation
method (EIM)

Parametric
maps

Appendix

Ex) Finite element (FE) dimension $\mathcal{N} = 3$,
Reduced basis (RB) dimension $N = 2$

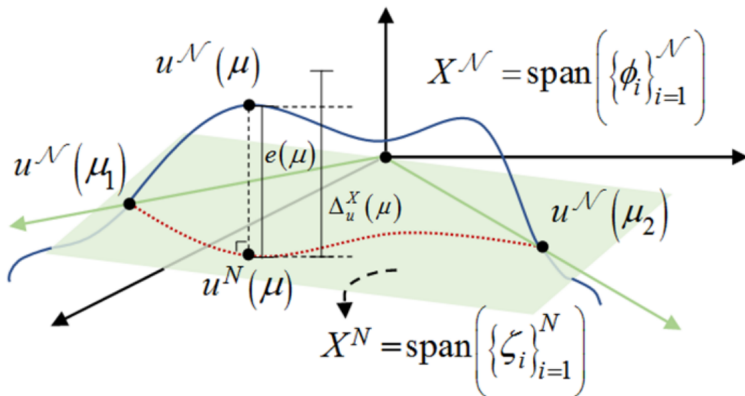


Figure 13: Concept of RB method[†]

[†] Kang, S., & Lee, K. (2021). Real-time, high-fidelity linear elastostatic beam models for engineering education. Journal of Mechanical Science and Technology, 35(8), 3483-3495.

Methods

Fatigue analysis

Fatigue analysis

Linear elasticity problem

Geometric parameterization

Empirical interpolation method (EIM)

Parametric maps

Steps for fatigue analysis in ASME Pressure Vessel Code[†]

- ① Determine the load history of the vessel.
- ② Determine the individual cycles and define the total number of cyclic stress ranges in the load history.
- ③ Determine the equivalent stress range for the cycle.
- ④ Determine the effective alternating equivalent stress amplitude for the cycle.
- ⑤ Determine the number of cycles to failure for the alternating equivalent stress.

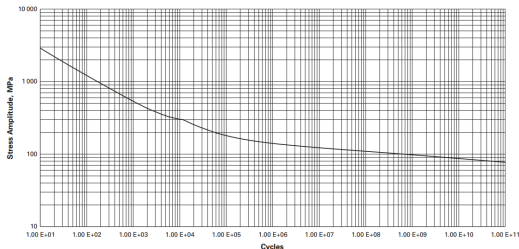


Figure 14: Fatigue curve of a vessel steel[†]

[†] The American Society of Mechanical Engineers, ASME Boiler & Pressure Vessel Code, Section VIII Division 2, 2019 Edition

Methods

Linear elasticity problem

- Strong form

$$\frac{\partial}{\partial x_j^0(\mu)} \left(C_{ijkl}^0(\mu) \frac{\partial u_k^0(\mu)}{\partial x_l^0(\mu)} \right) = 0, \quad \text{in } \Omega^0(\mu) \quad (4)$$

- Boundary conditions

$$u^0 = 0 \quad \text{on } \Gamma_1^0, \Gamma_2^0, \quad C_{ijkl}^0 \frac{\partial u_k^0}{\partial x_l^0} e_{n,j} = q e_{n,i} \quad \text{on } \Gamma_3^0 \quad (5)$$

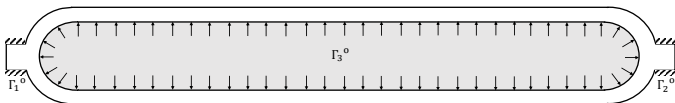


Figure 15: Boundary conditions of a damaged vessel model

- Computational subdomains

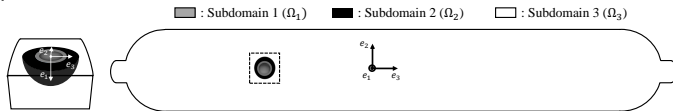


Figure 16: Computational subdomains of a damaged vessel

- Weak form

$$\sum_{s=1}^3 \int_{\Omega_s^0(\mu)} \frac{\partial v_i^0}{\partial x_j^0(\mu)} C_{ijkl}^0(\mu) \frac{\partial u_k^0(\mu)}{\partial x_l^0(\mu)} d\Omega^0(\mu) = \int_{\Gamma_3^0(\mu)} q^0(\mu) e_{n,i}^0(\mu) v_i^0 d\Gamma^0(\mu), \quad \forall v^0 \in X^0(\mu) \quad (6)$$

- Weak form in parameter-independent reference domain Ω

- Required to map geometric parameter μ_d efficiently
- Enabled by a Jacobian matrix J_Φ of a parametric map $\Phi(x; \mu)$

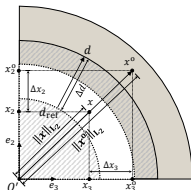
Methods

Geometric parameterization

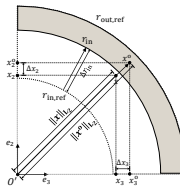
- Parametric map $\Phi(x; \mu) = x^0(x; \mu) = x + \Delta x_d(\mu)$
- Geometric parametrization for dent size μ_d
 - Transformation ratio: variate the dent size along the ratio $\frac{\mu_d - d_{\text{ref}}}{\|x\|_{L_2}}$
- Geometric parametrization for each subdomain

Subdomain 1: $x^0(x; \mu) = x + \frac{\mu_d - d_{\text{ref}}}{\|x\|_{L_2}} x$

Subdomain 2: $x^0(x; \mu) = x + \left(\frac{\mu_d - d_{\text{ref}}}{\|x\|_{L_2}} \right) \left(\frac{\|x\|_{L_2} - r_{\text{ref,out}}}{r_{\text{ref,in}} - r_{\text{ref,out}}} \right) x$



(a) Ω_1



(b) Ω_2

Figure 17: Schematic representation of mapping functions

- Weak form in a reference domain

$$\sum_{s=1}^3 \int_{\Omega_s} \frac{\partial v_i}{\partial x_j} C_{ijkl,s}(x; \mu) \frac{\partial u_k(\mu)}{\partial x_l} d\Omega = \int_{\Gamma_3} q(x; \mu) e_n v_i d\Gamma, \quad \forall v \in X, \quad (7)$$

where

$$C_{ijkl,s}(x; \mu) = [J_{\Phi_s}^{-1}(x; \mu)]_{jj'} C_{ij'kl'}^0(\mu) [J_{\Phi_s}^{-1}(x; \mu)]_{ll'} |J_{\Phi_s}(x; \mu)|,$$

$$q(x; \mu) = q^0(\mu) |J_{\Phi_3}(x; \mu) e_n|.$$

Results

Damage scenarios [1/2]

- Scenario 1: vessel with initially identified dent size $\mu_d=1$ cm (number of MCMC samples: 10^4)

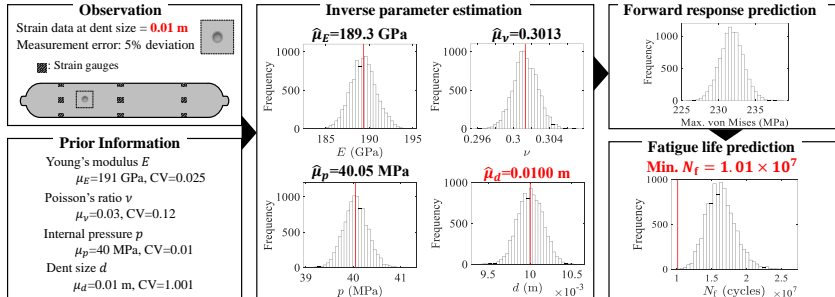


Figure 18: Statistical fatigue life prediction of a damaged vessel for scenario 1

Table 4: Posterior estimates and credible intervals for scenario 1

Parameters	True	Estimated mean	Estimated stdv	95% CI
E [GPa]	191	189.3	1.49	[186.40, 192.25]
ν [-]	0.3000	0.3013	0.0014	[0.2987, 0.3040]
p [MPa]	40	40.05	0.26	[39.55, 40.55]
d [m]	0.0100	0.0100	0.00015	[0.0097, 0.0103]

stdv: standard deviation, CI: credible interval

Results

6/8

Damage scenarios [2/2]

- Scenario 2: vessel with enlarged dent size $\mu_d=3$ cm (number of MCMC samples: 10^4)

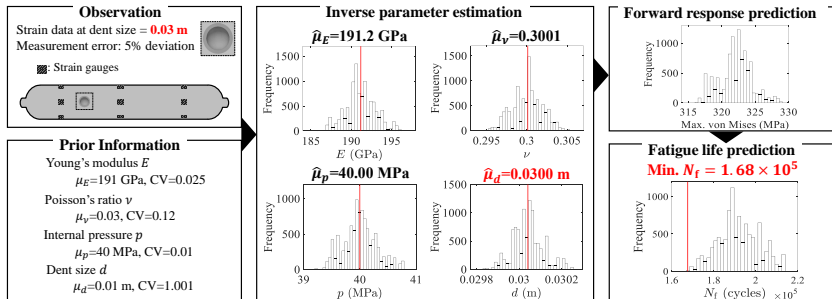


Figure 19: Statistical fatigue life prediction of a damaged vessel for scenario 2

Table 5: Posterior estimates and credible intervals for scenario 1

Parameters	True	Estimated mean	Estimated stdv	95% CI
E [GPa]	191	191.2	1.83	[187.60, 194.76]
ν [-]	0.3000	0.3001	0.0019	[0.2964, 0.3038]
p [MPa]	40	40.00	0.29	[39.43, 40.56]
d [m]	0.0300	0.0300	0.00007	[0.0299, 0.0302]

stdv: standard deviation, CI: credible interval

- Used to ensure affine parametric dependence for an offline/online decomposition in RB analysis

$$\underbrace{\sum_{q=1}^{Q_a} \theta_a^q(\mu) \underbrace{\mathbb{B}^T A_{\mathcal{N}}^q \mathbb{B}}_{\text{offline}} u_N(\mu)}_{\text{online}} = \sum_{q=1}^{Q_f} \theta_f^q(\mu) \underbrace{\mathbb{B}^T f_{\mathcal{N}}^q}_{\text{offline}}$$

- Approximated non-affine function to affine function by

$$\begin{aligned} \Phi(x; \mu) &= M_{EIM}(x; \mu) + e_{EIM}(x; \mu) \\ &= \sum_{j=1}^Q \theta_j(\mu) h_j(x) + e_{EIM}(x; \mu) \end{aligned}$$

$\theta(\mu)$: interpolation coefficients

$h(x)$: EIM basis functions

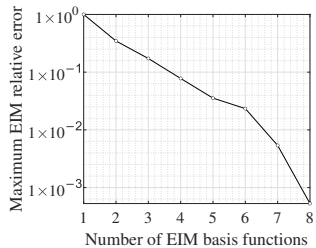


Figure 20: Error convergence for EIM training

- Applied to a vessel problem due to non-affine mapping functions represented as:

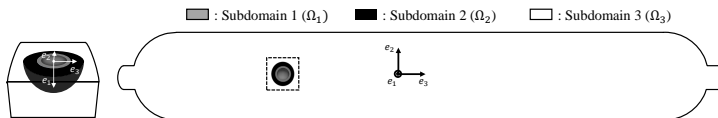


Figure 21: Computational subdomains of a damaged vessel

Table 2: Parametric maps on subdomains

Subdomain	Parametric map $M(x; \mu)$
Ω_1	$\begin{bmatrix} x_1^o \\ x_2^o \\ x_3^o \end{bmatrix} = \begin{bmatrix} x_1 + (x_1 - x_{1,0}) \frac{(\mu_4 - d_{\text{ref}})}{\ x\ _{L_2}} \\ x_2 + (x_2 - x_{2,0}) \frac{(\mu_4 - d_{\text{ref}})}{\ x\ _{L_2}} \\ x_3 + (x_3 - x_{3,0}) \frac{(\mu_4 - d_{\text{ref}})}{\ x\ _{L_2}} \end{bmatrix}$
Ω_2	$\begin{bmatrix} x_1^o \\ x_2^o \\ x_3^o \end{bmatrix} = \begin{bmatrix} x_1 + (x_1 - x_{1,0}) \left(\frac{\ x\ _{L_2} - r_{\text{ref,out}}}{r_{\text{ref,in}} - r_{\text{ref,out}}} \right) \\ x_2 + (x_2 - x_{2,0}) \left(\frac{\ x\ _{L_2} - r_{\text{ref,out}}}{r_{\text{ref,in}} - r_{\text{ref,out}}} \right) \\ x_3 + (x_3 - x_{3,0}) \left(\frac{\ x\ _{L_2} - r_{\text{ref,out}}}{r_{\text{ref,in}} - r_{\text{ref,out}}} \right) \end{bmatrix} \begin{bmatrix} \frac{(\mu_4 - d_{\text{ref}})}{\ x\ _{L_2}} \\ \frac{(\mu_4 - d_{\text{ref}})}{\ x\ _{L_2}} \\ \frac{(\mu_4 - d_{\text{ref}})}{\ x\ _{L_2}} \end{bmatrix}$
Ω_3	$\begin{bmatrix} x_1^o \\ x_2^o \\ x_3^o \end{bmatrix} = \begin{bmatrix} x_1 \\ x_2 \\ x_3 \end{bmatrix}$